Superdeformed structures in ^{197,198}Pb

I. M. Hibbert,[1] R. Wadsworth,[1] K. Hauschild,[1] H. Hübel,[2] W. Korten,[2] U. J. van Severen,[2] E. S. Paul,[3] A. N. Wilson,[3] J. N. Wilson,[3,*] A. P. Byrne,[4] W. Satuła,[5,6] and R. Wyss[5]

[1]*Department of Physics, University of York, Heslington, York, Y01 5DD, United Kingdom*
[2]*Institut für Strahlen-und Kernphysik, Universität Bonn, Nussallee 14-16, D-53115 Bonn, Germany*
[3]*Oliver Lodge Laboratory, University of Liverpool, PO Box 147, Liverpool, L69 3BX, United Kingdom*
[4]*Department of Nuclear Physics, Australian National University, Canberra ACT 0200, Australia*
[5]*Manne Siegbahn Institute of Physics, Frescativägen 24, S-104 05 Stockholm, Sweden*
[6]*Institute of Theoretical Physics, University of Warsaw, ul. Hoża 69, PL-00 681 Warsaw, Poland*

(Received 1 May 1996)

Two new superdeformed bands, which possess almost constant dynamic moments of inertia as a function of rotational frequency, have been observed in ^{197}Pb. They are thought to be based upon the favored and unfavored signature components of an $N=7$ neutron intruder orbital. Previous work tentatively assigned a superdeformed band to ^{198}Pb. The present work has confirmed this assignment. The properties of all the bands are discussed in terms of extended total Routhian surface calculations. [S0556-2813(96)00311-1]

PACS number(s): 21.10.Re, 21.60.Ev, 23.20.Lv, 27.80.+w

I. INTRODUCTION

Superdeformation (SD) is now well established in the $A\sim 190$ mass region [1,2]. The vast majority of the SD bands in this region show a similar behavior of their dynamic moment of inertia ($\mathcal{J}^{(2)} = dI/d\omega$) with rotational frequency (ω), in that they exhibit a smooth rise as ω increases. This is calculated [3,4] to result from the gradual alignment of pairs of nucleons occupying high-N intruder orbitals (namely, $j_{15/2}$ neutrons and $i_{13/2}$ protons) in the presence of pairing correlations. The Pauli blocking of the high-N intruder orbitals, which should reduce the increase in the dynamic moment of inertia, is used to explain the behavior of certain SD bands in ^{193}Hg [5], ^{193}Pb [6], and ^{195}Pb [7], where the $\mathcal{J}^{(2)}$ curve is somewhat flatter than that of most of the bands in this region. Furthermore, in the odd-odd isotopes: ^{196}Bi [8], ^{192}Tl [9], and ^{194}Tl [10], the almost constant $\mathcal{J}^{(2)}$ is explained by double blocking of both the quasineutron and quasiproton alignments. The heaviest known lead isotope with a confirmed SD band is ^{196}Pb [11]; however, there are tentative reports of a band in ^{198}Pb [12,13].

Results are presented here of the discovery of two, very weakly populated SD bands in ^{197}Pb. Total Routhian surface (TRS) calculations, in which the $j_{15/2}$ neutron orbital is blocked, can account for the observed, almost constant, dynamic moment of inertia. The present work is also able to unambiguously verify the assignment of the previously reported SD band in ^{198}Pb [12,13]. Thus it has been possible to extend the region of known SD bands in the lead isotopes. The results obtained are discussed in terms of recent cranking calculations, and comparisons are made with other SD bands seen in this mass region.

II. EXPERIMENTAL PROCEDURE

High spin states in ^{197}Pb and ^{198}Pb nuclei were produced in the $7n$ and $6n$ channels of the ^{186}W (^{18}O,xn) reaction at nominal laboratory bombarding energies of 110 and 115 MeV. The beam from the Vivitron electrostatic accelerator at the Centre de Recherches Nucléaires in Strasbourg was incident upon a target consisting of 3×200 μg/cm^2 stacked foils of ^{186}W mounted on thin (20 μg/cm^2) carbon backings. Gamma rays were detected with the EUROGAM phase 2 spectrometer [14], consisting of 30 large-volume escape-suppressed Ge detectors [15], 15 at the forward and 15 at the backward angles, and 24 Clover detectors [16] at angles near 90° to the beam direction. The Clover detectors have four closely packed Ge detectors sharing the same cryostat, surrounded by a single escape-suppression shield.

III. DATA ANALYSIS AND EXPERIMENTAL RESULTS

In the 3 day experiment, a total of 1.2×10^9 events were collected in which at least four γ rays were in prompt time coincidence (with a hardware coincidence time window of $\leqslant$50 ns). The data were unpacked into triple-coincidence events using the technique given in Ref. [17] and analyzed off line by sorting these events into $E_{\gamma 1}$-$E_{\gamma 2}$-$E_{\gamma 3}$ RADWARE format [18] cubes. A systematic search of the cube containing data from the 115 MeV data set revealed the presence of two cascades of γ rays with an energy spacing of $\Delta E_\gamma\sim 40$ keV. A γ-γ-gated $E_{\gamma 1}$-$E_{\gamma 2}$ matrix for each band was then produced, from which triple-gated spectra were obtained (Fig. 1). All in-band transitions were used as gates to construct these spectra. The relative intensities of all transitions, corrected for $E2$ internal conversion, are shown as an inset.

The two bands, which were observed with an intensity of $\sim$0.2 % and 0.1 %, respectively, of the ^{197}Pb reaction channel, have been assigned to ^{197}Pb as they are observed in coincidence with lead x rays and several low-lying states in

*Present address: Department of Physics and Astronomy, McMaster University, Hamilton, ON, Canada L8S 4M1.

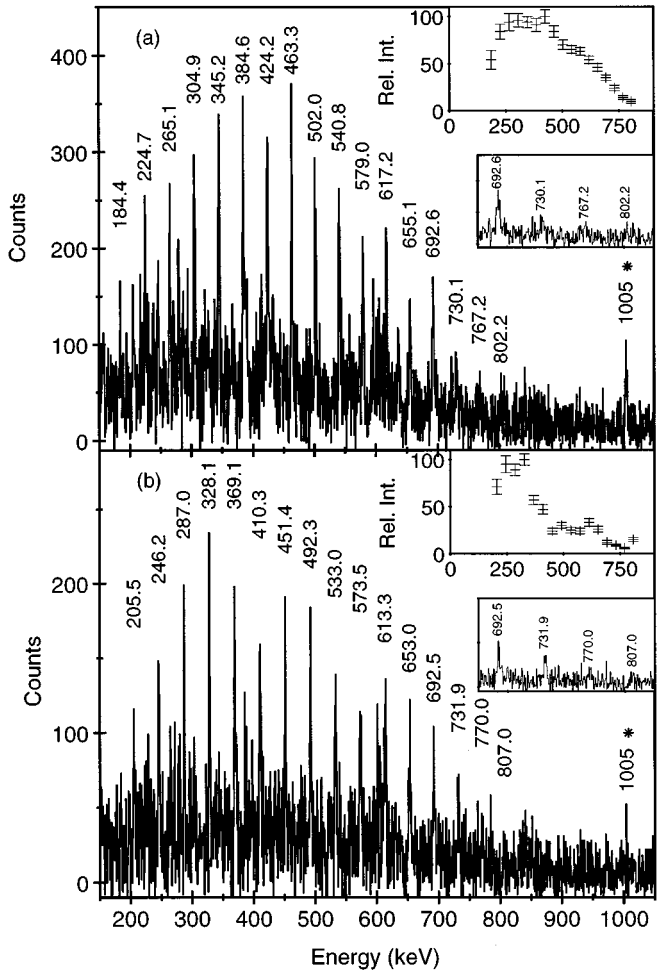

FIG. 1. Triple-gated quadruples spectra of the two superdeformed bands in ^{197}Pb, with gates set on all the known transitions in the band. Insets show the relative transition intensities, corrected for $E2$ internal conversion, as a percentage of the largest peak intensity in the band. Also shown is the 1005 keV γ ray from ^{197}Pb.

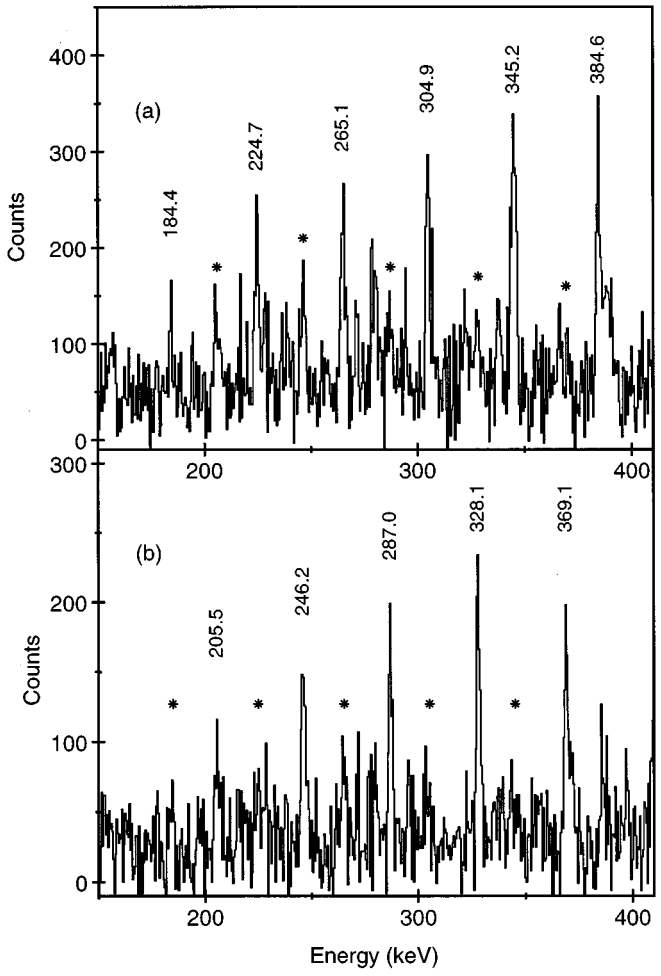

FIG. 2. Evidence for the crosstalk between the two superdeformed bands in ^{197}Pb: spectra formed from the sum of gates of transitions in (a) band 1, and (b) band 2, with locations of transitions in the signature partner band given by ⋆.

this nucleus [19], including the 1005 keV γ ray ($17/2^+ \rightarrow 13/2^+$, 43 min isomer). These bands are seen more strongly in the 115 MeV data set than in that obtained with a bombarding energy of 110 MeV, where the production of ^{198}Pb dominates. Evidence that these bands are signature partners and share a similar structure is presented in Fig. 2, where crosstalk is seen between the bands. Lower band members from band 2 are seen in the sum of gates of band 1 in ^{197}Pb and vice versa, with an intensity that decreases as the rotational frequency increases.

At the lower beam energy, where the population of ^{198}Pb dominates, another weakly populated SD band was observed ($\sim$0.5 % of the ^{198}Pb cross section). This band had previously been assigned to ^{198}Pb [12,13], but the assignment was not convincing due to the low intensity of the band. The present work unambiguously confirms that the band belongs to this nucleus. A double-gated γ-ray spectrum formed from the sum of uncontaminated band members from the 110 MeV data is shown in Fig. 3. This band is seen in coincidence with lead x rays and known low-lying states in ^{198}Pb [20], most notably the 541 keV ($10^+ \rightarrow 9^-$) and 929 keV ($14^+ \rightarrow 12^+$, 212 ns isomer) transitions. This band is

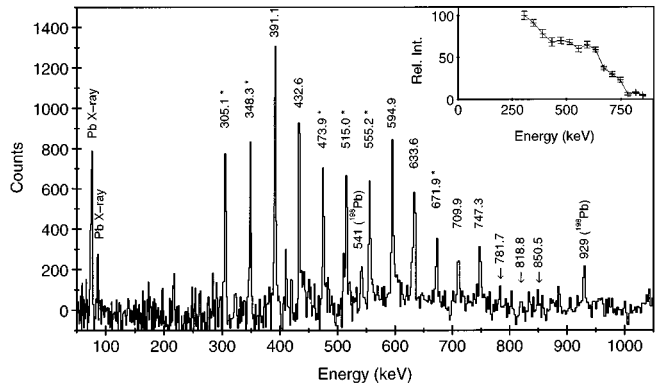

FIG. 3. Coincidence spectrum obtained using triples data for the SD band in ^{198}Pb, produced by setting double gates on combinations of all transitions marked with asterisk. Transition energies are labeled in keV, along with the 541 and 929 keV transitions from ^{198}Pb, and Pb x rays. Also shown is the relative transition intensity corrected for $E2$ internal conversion, obtained from a sum of all known gates.

reduced in absolute intensity at the higher beam energy where the population of ^{197}Pb dominates the reaction cross section. The relative intensity profile, corrected for $E2$ internal conversion, shows that there seems to be an extremely rapid depopulation of the band: no transitions are observed in the band with energies below 305 keV. The transition of highest spin in the normal deformed well which is observed in coincidence with the band is 929 keV from the $I^{\pi}=14^{+}$ level. This would suggest a spin of $\sim 16\hbar$ or higher for the lowest state in the band. However, a spin of $12\hbar$ is obtained for the lowest state in the band using the spin fitting technique of Ref. [21]. This is clearly somewhat lower than the value suggested by the experimental data.

Because of the very weak population intensity of all three bands, it was not possible to perform an angular correlation analysis. However, as the properties of the γ rays are very similar to those in other known SD bands in the lighter lead isotopes, it assumed that the bands are composed of stretched electric quadrupole transitions.

IV. DISCUSSION

A. ^{197}Pb

Extended total Routhian surface calculations have been performed for the SD bands of the Pb region. In these calculations, pairing and deformation are treated self-consistently by means of the cranked Strutinsky Lipkin-Nogami approach [22]. Second-order residual interactions were introduced using a quadrupole pairing term in the Hamiltonian. These calculations can account for the moments of inertia of a broad range of nuclei in this mass region [22–24] as well as for selected blocked configurations of odd and odd-odd nuclei [25]. In general, the $\mathcal{J}^{(2)}$ moments of inertia exhibit a smooth increase with frequency. Therefore, it is a challenge to the model to see how well the observed flat moments of inertia of SD bands in odd-N Pb nuclei can be reproduced. In addition, it is possible to investigate to what extent the previous assignments appear reasonable.

The dynamic moments of inertia for the two bands in ^{197}Pb are plotted in Fig. 4, along with those of bands 1 and 2 in ^{195}Pb [7]. These bands are thought to be based upon the odd neutron occupying either the favored or unfavored signature components of an $N=7$ neutron intruder orbital. The expected alignment of $j_{15/2}$ neutrons is then prevented by Pauli blocking, producing a relatively constant moment of inertia. A pair of similar bands has also been reported in ^{193}Pb [6]. However, because there is less fission competition in the ^{197}Pb system, the new bands are observed to extend to higher rotational frequencies than those seen in the lighter nuclei.

Calculated dynamic moments of inertia are shown in Fig. 5. They show the contribution to $\mathcal{J}^{(2)}$ of the high-N neutron and proton orbitals that lie close to the Fermi surface at superdeformation. In these calculations, the two $N=7$ states are the lowest neutron orbitals and can be blocked self-consistently. The unfavored $N=7$ state is crossed at $\hbar\omega=0.35$ MeV by an $N=5$ orbital, that is mixed and contains contributions from a partially aligned pair of $N=7$ neutrons. Beyond this point, it is impossible to trace the unfavored $N=7$ orbital. Nevertheless, the calculations clearly

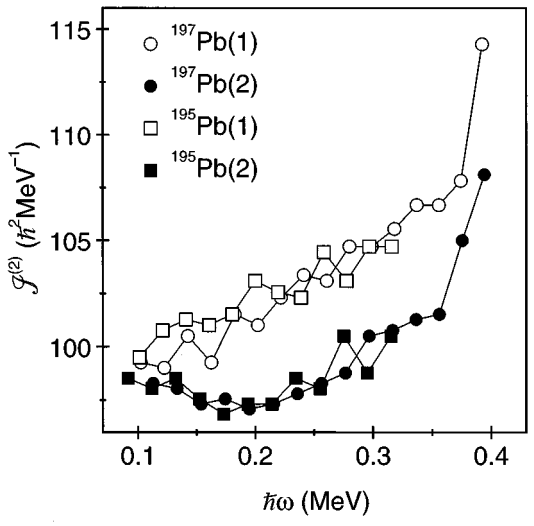

FIG. 4. Dynamic moment of inertia plotted as a function of rotational frequency for the two new SD bands in ^{197}Pb compared with the $\mathcal{J}^{(2)}$ for bands 1 and 2 in ^{195}Pb [7].

reveal that, due to the blocking of a single $N=7$ orbital, the neutron contribution to $\mathcal{J}^{(2)}$ is essentially constant.

Both the new bands in ^{197}Pb show a small rise in $\mathcal{J}^{(2)}$ at $\hbar\omega\sim 0.37$ MeV (Fig. 4). This agrees well with the calculations although the calculated proton alignment appears smoother than in experiment. It would appear however, that the neutron $N=7$ and $N=5$ level crossing is not observed experimentally. Since the protons do not start to align their angular momenta until $\hbar\omega\sim 0.35$ MeV, this results in an almost flat total moment of inertia at lower frequencies where the neutron alignment is blocked. The SD bands in the lighter nuclei, ^{193,195}Pb, are not observed to as high a rota-

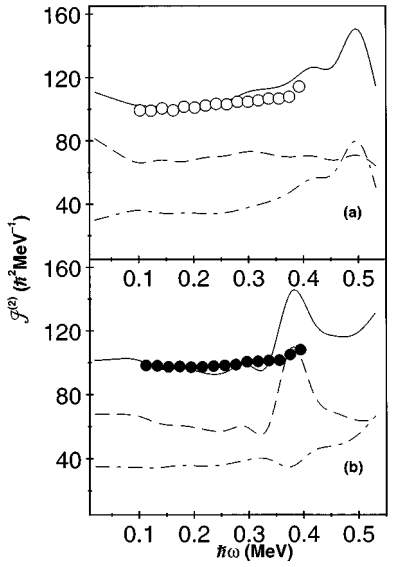

FIG. 5. Dynamic moments of inertia plotted as a function of rotational frequency for the two new SD bands in ^{197}Pb compared with the calculated proton (dot-dashed line), neutron (dashed), and total (solid) $\mathcal{J}^{(2)}$ for configurations involving occupation of the (a) favored ($\alpha=-1/2$) and (b) unfavored ($\alpha=+1/2$) signatures of an $N=7$ intruder orbital.

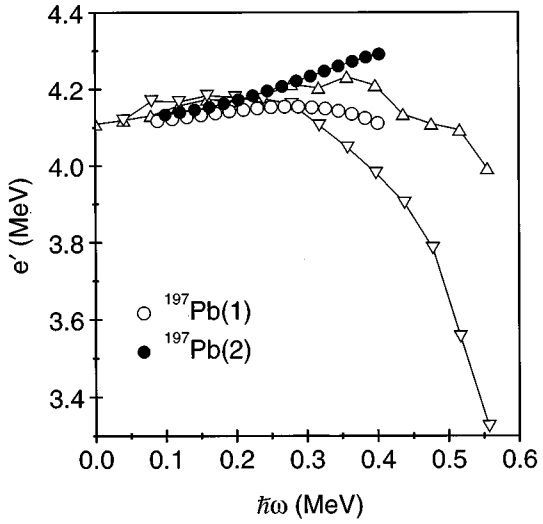

FIG. 6. Experimental Routhians for the SD bands in ^{197}Pb (circles) after a rigid rotor reference with the Harris parameters $J_0=100.0\hbar^2$/MeV and $J_1=0.1\hbar^4$/MeV^3 had been subtracted. These are compared to total Routhian surface calculations with $A=197$ and the unpaired neutron occupying: the favored ($\alpha=-1/2$) signature of an $N=7$ intruder orbital ($\triangle$) and the unfavored ($\alpha=+1/2$) signature ($\triangledown$).

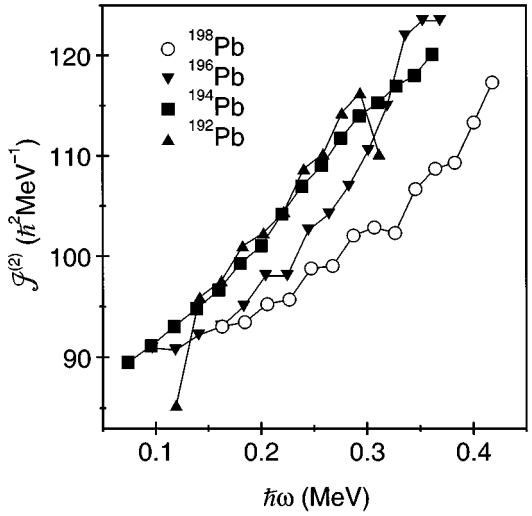

FIG. 7. Comparison of experimental dynamic moment of inertia for ^{198}Pb with experimental $\mathcal{J}^{(2)}$ for yrast SD bands in even-even Pb isotopes.

tional frequency as the ^{197}Pb bands, so the $i_{13/2}$ proton alignment remains unobserved. The proton alignment depends sensitively on deformation, where the gain in alignment increases with decreasing deformation. The odd-N Pb isotopes are predicted to belong to the most deformed SD nuclei in this mass region, having a larger deformation (by $\sim$ 2–3 %) than the corresponding Hg isotopes. The predicted increase in deformation going from Hg to Pb isotopes could also explain why the crossing between the $N=7$ and $N=5$ orbitals remains unobserved in the odd-mass Pb nuclei.

A comparison of calculated and experimental Routhians is presented in Fig. 6. The good agreement of the calculated $\mathcal{J}^{(2)}$ with experiment gives confidence to take those spin values that agree best with the calculations. Since the spins can only be changed in steps of two $\hbar$, these assignments seem rather well justified. Thus the 184.4 keV transition in band 1 ($\alpha=-1/2$) is assigned as $19/2 \rightarrow 15/2$, and the 205.5 keV γ ray from band 2 ($\alpha=+1/2$) as $21/2 \rightarrow 17/2$. These values agree with results obtained using the method of [21]. The relative excitation energy of band 1 to band 2 has not been determined experimentally, and so an arbitrary offset has been applied to each Routhian so that the e' extrapolate to the same value at $\hbar\omega = 0$ MeV.

An interesting feature of the present data is that the transition energies of the signature partner bands in ^{197}Pb become very similar beyond 650 keV. Band 2 has approximately the midpoint energies of transitions in band 1 at low frequency, but almost identical energies near the top of the band. The onset of a similar effect is also observed in ^{195}Pb, where the last two transitions in the $j_{15/2}$ bands are 612.7, 650.9 keV ($\alpha=-1/2$) and 610.8, 650.6 keV ($\alpha=+1/2$), respectively. This feature can be explained qualitatively by the behavior of the theoretical Routhians, e' (Fig. 6). The curvature of e' is related to the dynamic moment of inertia: the greater curvature for the favored signature (band 1, $\alpha=-1/2$) results in a larger $\mathcal{J}^{(2)}$, as observed experimentally (Fig. 4). At low frequency, there is essentially no signature splitting present for the $j_{15/2}$ states. Then, with increasing frequency, for $\hbar\omega>0.2$ MeV, the Coriolis coupling mixes in $\Omega=1/2$ components into the $j_{15/2}$ orbital, and the signature splitting increases with frequency. The signature splitting also rules out assignments in terms of the high-Ω orbitals, that are close to the Fermi surface. The signature splitting is further in agreement with observed intensities, where the greater feeding is expected for the yrast band. The fact that the bands have comparable γ ray energies around the highest observed frequencies implies that the difference in aligned angular momentum corresponds to exactly one unit of $\hbar$.

B. ^{198}Pb

The dynamic moment of inertia for the SD band in ^{198}Pb (Fig. 7) is not as flat as the moments of inertia of the two new bands in ^{197}Pb in the frequency range $\hbar\omega\sim0.2$–0.35 MeV, however it is clearly much flatter than that of the yrast SD bands in ^{192,194,196}Pb [2]. This suggests that there may be a reduced or delayed alignment for the $j_{15/2}$ neutrons in ^{198}Pb. Although the calculations can reproduce the experimentally observed $\mathcal{J}^{(2)}$ for many Hg-Pb nuclei over a wide frequency range [23–25], the agreement for ^{198}Pb is not satisfactory. The calculated values of $\mathcal{J}^{(2)}$ at low frequency are in agreement with experiment (Fig. 8). However, above $\hbar\omega\approx0.2$ MeV, the theoretical $j_{15/2}$ neutron alignment is considerably more pronounced. Calculations are also shown where the lowest two-quasiparticle configuration ($\pi,\alpha=-,0$) is blocked. These yield an essentially flat moment of inertia, followed by a rather sharp crossing at $\hbar\omega\approx0.35$ MeV, where there is a shape change from $\beta_2=0.48$ to $\beta_2=0.44$, with an accompanied gain in alignment for both protons and neutrons. This is due to a balance between shell structure, which favors larger deformation, and alignment gain, which pushes the nucleus into a smaller deformed region. The TRS corresponding to this two-

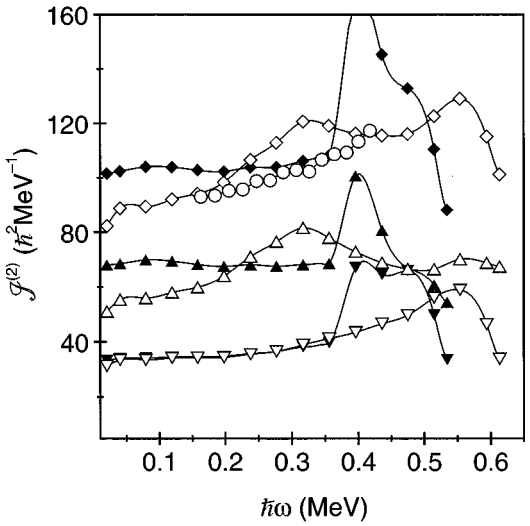

FIG. 8. Comparison of experimental $\mathcal{J}^{(2)}$ for ^{198}Pb (○) with results from extended TRS calculations with the Harris parameters $J_0=90.0\hbar^2$/MeV and $J_1=0.0\hbar^4$/MeV^3 for ^{198}Pb that show the proton (▽), neutron (△) and total (◇) $\mathcal{J}^{(2)}$ contributions. Unfilled symbols correspond to the ground-state configuration, while filled symbols represent the two-quasiparticle configuration ($\pi,\alpha=-,0$).

quasiparticle configuration is calculated to be higher in energy than the corresponding ground-state configuration and hence it might be expected that the two-quasiparticle configuration would not be observed at all. The experimentally observed smooth alignment may indicate the presence of correlations that are not taken into account in this model, such as the coupling to vibrational phonon states or low-lying octupole vibrational bands which have been calculated for Hg isotopes [26]. Another possibility would be that the shell gap at $N=116$ is more pronounced than the model predicts.

V. CONCLUSION

Two new SD bands have been identified in ^{197}Pb and are assigned to the favored and unfavored signatures of an $N=7$ neutron intruder orbital. The expected alignment of $j_{15/2}$ neutrons is then prevented by Pauli blocking, producing flat moments of inertia, similar to those seen in bands in ^{193,195}Pb. The calculated blocking effect suggests that the odd-N SD Pb isotopes have a larger deformation than the corresponding Hg isotones. The enhanced deformation delays the proton alignment and accounts for the different alignment pattern of the odd Hg and Pb isotones. The tentative assignment of a SD band to ^{198}Pb has also been confirmed, thus extending the region where superdeformation is known in nuclei with $A\sim190$. Work is continuing to search this mass region for more SD bands so as to give a greater understanding of the role of pairing correlations and Pauli blocking effects in these nuclei, in order to test current mean field nuclear models.

ACKNOWLEDGMENTS

The EUROGAM is jointly funded by the EPSRC (UK) and IN2P3 (France). This work was supported in part by the EPSRC, (A.N.W. and J.N.W.). K.H. acknowledges support from the University of York. W.S. acknowledges support from the Göran Gustafsson Foundation and R.W. from the Swedish Natural Research Council (NFR). The work of the Bonn group was supported by BMBF (Germany). We also wish to thank the crew and staff of the Vivitron, CNRS, Strasbourg, R. Darlington of Daresbury who manufactured the targets, and D.C. Radford for providing the RADWARE analysis software.

[1] R.V.F. Janssens and T.L. Khoo, Annu. Rev. Nucl. Part. Sci. **41**, 321 (1991).

[2] B. Singh, R.B. Firestone, and S.Y.F. Chu, ''Table of Superdeformed Nuclear Bands and Fission Isomers,'' LBL Report No. LBL-38004 (unpublished).

[3] M.A. Riley, D.M. Cullen, A. Alderson, I. Ali, P. Fallon, P.D. Forsyth, F. Hanna, S.M. Mullins, J.W. Roberts, J.F. Sharpey-Schafer, P.J. Twin, R. Poynter, R. Wadsworth, M.A. Bentley, A.M. Bruce, J. Simpson, G. Sletten, W. Nazarewicz, T. Bengtsson, and R. Wyss, Nucl. Phys. **A512**, 178 (1990).

[4] M.W. Drigert, M.P. Carpenter, R.V.F. Janssens, I. Ahmad, P.B. Fernandez, E.F. Moore, T.L. Khoo, F.L.H. Wolfs, D. Ye, K.B. Beard, U. Garg, and Ph. Benet, Nucl. Phys. **A530**, 452 (1991).

[5] M.J. Joyce, J.F. Sharpey-Schafer, M.A. Riley, D.M. Cullen, F. Azaiez, C.W. Beausang, R.M. Clark, P.J. Dagnall, I. Deloncle, J. Duprat, P. Fallon, P.D. Forsyth, N. Fotiades, S.J. Gale, B. Gall, F. Hannachi, S. Harissopulos, K. Hauschild, P.M. Jones, C.A. Kalfas, A. Korichi, Y. Le Coz, M. Meyer, E.S. Paul, M.-G. Porquet, N. Redon, C. Schück, J. Simpson, R. Vlastou, R. Wadsworth, and W. Nazarewicz, Phys. Lett. **B340**, 150 (1994).

[6] J.R. Hughes, J.A. Becker, L.A. Bernstein, M.J. Brinkman, L.P. Farris, E.A. Henry, R.W. Hoff, M.A. Stoyer, D.T. Vo, S. Asztalos, B. Cederwall, R.M. Clark, M.A. Deleplanque, R.M. Diamond, P. Fallon, I.Y. Lee, A.O. Macchiavelli, and F.S. Stephens, Phys. Rev. C **51**, R447 (1995).

[7] L.P. Farris, E.A. Henry, J.A. Becker, M.J. Brinkman, B. Cederwall, J.A. Cizewski, M.A. Deleplanque, R.M. Diamond, J.E. Draper, C. Duyar, P. Fallon, J.R. Hughes, W.H. Kelly, I.Y. Lee, A.O. Macchiavelli, E.C. Rubel, F.S. Stephens, M.A. Stoyer, and D.T. Vo, Phys. Rev. C **51**, 2288 (1995).

[8] R.M. Clark, S. Bouneau, A.N. Wilson, B. Cederwall, F. Azaiez, S. Asztalos, J.A. Becker, L. Bernstein, M.J. Brinkman, M.A. Deleplanque, I. Deloncle, R.M. Diamond, J. Duprat, P. Fallon, L.P. Farris, E.A. Henry, J.R. Hughes, W.H. Kelly, I.Y. Lee, A.O. Macchiavelli, M.-G. Porquet, J.F. Sharpey-Schafer, F.S. Stephens, M.A. Stoyer, and D.T.Vo, Phys. Rev. C **53**, 117 (1995).

[9] Y. Liang, M.P. Carpenter, R.V.F. Janssens, I. Ahmad, R.G.

Henry, T.L. Khoo, T. Lauritsen, F. Soramel, S. Pilotte, J.M. Lewis, L.L. Riedinger, C.-H. Yu, U. Garg, W. Reviol, and I.G. Bearden, Phys. Rev. C **46**, R2136 (1992).

[10] F. Azaiez, W.H. Kelly, W. Korten, F.S. Stephens, M.A. Deleplanque, R.M. Diamond, A.O. Macchiavelli, J.E. Draper, E.C. Rubel, C.W. Beausang, J. Burde, J.A. Becker, E.A. Henry, S.W. Yates, M.J. Brinkman, A. Kuhnert, and T.F. Wang, Phys. Rev. Lett. **66**, 1030 (1991).

[11] U.J. van Severen, W. Korten, H. Hübel, D. Bazzacco, G. Lo Bianco, N.H. Medina, C. Rossi Alvarez, S. Signorelli, K. Strähle, and P. Willsau, Z. Phys. A **353**, 15 (1995).

[12] T.F. Wang, A. Kuhnert, J.A. Becker, E.A. Henry, S.W. Yates, M.J. Brinkman, J.A. Cizewski, F. Azaiez, M.A. Deleplanque, R.M. Diamond, J.E. Draper, W.H. Kelly, W. Korten, A.O. Macchiavelli, E. Rubel, and F.S. Stephens, Phys. Rev. C **43**, R2465 (1991).

[13] R.M. Clark, R. Wadsworth, K. Hauschild, I.M. Hibbert, E. Dragulescu, C.W. Beausang, M.H. Bergstrom, S. Clarke, P.J. Dagnall, P.M. Jones, E.S. Paul, A.T. Semple, J.F. Sharpey-Schafer, J. Simpson, W. Satuła, and R. Wyss, Phys. Rev. C **50**, 1222 (1994).

[14] P.J. Nolan, F.A. Beck, and D.B. Fossan, Annu. Rev. Nucl. Part. Sci. **45**, 561 (1994).

[15] C.W. Beausang, S.A. Forbes, P. Fallon, P.J. Nolan, P.J. Twin, J.N. Mo, J.C. Lisle, M.A. Bentley, J. Simpson, F.A. Beck, D. Curien, G. de France, G. Duchêne, and D. Popescu, Nucl. Instrum. Methods A **313**, 37 (1992).

[16] G. Duchêne, ''International Conference on Nuclear Structure at High Angular Momentum,'' Chalk River Report AECL 10613, 1992, Vol. 2, p. 364.

[17] C.W. Beausang, D. Prevost, M.H. Bergstrom, G. de France, B. Haas, J.C. Lisle, Ch. Theisen, J. Timár, P.J. Twin, and J.N. Wilson, Nucl. Instrum. Methods A **364**, 560 (1995).

[18] D.C. Radford, Nucl. Instrum. Methods A **361**, 297 (1995).

[19] M. Pautrat, J.M. Lagrange, J.S. Dionisio, Ch. Vieu, and J. Vanhorenbeeck, Nucl. Phys. **A443**, 172 (1985).

[20] K. Honkanen, C.J. Herrlander, B. Fant, and T. Lönnroth, Nucl. Phys. **A451**, 141 (1986).

[21] J.A. Becker, E.A. Henry, A. Kuhnert, T.F. Wang, S.W. Yates, R.M. Diamond, F.S. Stephens, J.E. Draper, W. Korten, M.A. Deleplanque, A.O. Macchiavelli, F. Azaiez, W.H. Kelly, J.A. Cizewski, and M.J. Brinkman, Phys. Rev. C **46**, 889 (1992).

[22] W. Satuła and R. Wyss, Phys. Scr. **T56**, 159 (1995).

[23] W. Satuła and R. Wyss, Phys. Rev. C **50**, 2888 (1994).

[24] W. Satuła and R. Wyss, ''Conference on Physics from Large Gamma-Ray Detector Arrays,'' LBL Report LBL-35697, 1994, Vol. 2, p. 171.

[25] R. Wyss and W. Satuła, Phys. Lett. B **351**, 393 (1995).

[26] B. Crowell, M.P. Carpenter, R.V.F. Janssens, D.J. Blumenthal, J. Timár, A.N. Wilson, J.F. Sharpey-Schafer, T. Nakatsukasa, I. Ahmad, A. Astier, F. Azaiez, L. Du Croix, B.J.P. Gall, F. Hannachi, T.L. Khoo, A. Korichi, T. Lauritsen, A. Lopez-Martens, M. Meyer, D. Nisius, E.S. Paul, M.-G. Porquet, and N. Redon, Phys. Rev. C **51**, R1599 (1995).